Assessment of Highly Performance Secure Optical Communication Systems based on Chaotic Design

Nesreen M. Al-Saidi[*], Mudhafar H. Ali[**]

[*,**]*Computer Engineering Department, College of Engineering, Al-Iraqia University, Baghdad, Iraq*
[*]*nesreen.mohammed80@gmail.com*, [**]*mudhafar.ali@aliraqia.edu.iq*

Abstract

As optical communication system deployment is expensive, and reconfiguration is occasionally impossible or costly, system experiments and simulations have become necessary for predicting and optimizing system performance. OptiSystem is a cutting-edge optical communication simulation tool for designing, testing, and optimizing nearly any kind of optical connection in the physical layer of a wide range of optical systems. This paper proposed single-mode fiber as a transmitting medium for encrypted data. We examined a Dense Wavelength Division Multiplexing (DWDM) system with eight channels operating at 10 Gbps. A large capacity 80 Gbps system with a frequency range of 193.1 THz–193.8 THz and a Non-Return to Zero (NRZ) modulation format is analyzed in the proposed design. The results show that the proposed scheme can effectively transmit secure data based on new chaotic systems. MATLAB is used to implement the encryption and decryption processes, whereas some statistical analysis and OptiSystem 7 are used to assess the signal transmission in optical fibers. The performance of the proposed system is evaluated in terms of Quality Factor (Q-factor), Bit Error Rate (BER) and eye .diagram. It is observed that by varying the input power from -15 dBm to 15 dBm with step of 5 dBm, a low BER with a high Q-factor has the best values at 5 dBm of input signal power , where the maximum Q-factor is 42.2797, and the minimum BER of 0 is obtained for 100 km of optical fiber length. A slightly degradation in system performance was observed with increasing of fiber length from 50 km to 125 km.

Keywords- Fiber optic, DWDM, chaotic stream segmentation (CSS), stream ciphers, Optisystem simulation programs.

I. INTRODUCTION

Optical technology is becoming more critical for information security. Recent studies show that there has been an increase interest in the development of optical security methods. Chaotic encryption technique is used to encrypt the signal transferred in optical communication channel to ensure secure data communication, due to some of their important properties, which are unpredictable and noise-like signals. Communications using a chaotic carrier are difficult to intercept, where in optical communication, they are used as wideband carriers, which means that a lot of data can be sent at a fast rate. Most of previous strategies were based on encrypting and decrypting of the optical signals. For instance, Lilin Yi et al. [1] utilized Stimulated Brillouin Scattering (SBS) to encrypt and decrypt high-speed optical signals. Javidi et al. [2] proposed the Double-Random Phase Mask (DRPM) as an encryption process. Gao *et al.* [3] proposed method a novel optical phase encryption that individually encrypts each symbol with a differential-phase-shift-keying modulated (DPSK) method. Alapatt et al. [4] proposed a novel encryption system based on the Advanced Encryption Standard (AES).

Many studies are concerned with ensuring security for optical communications based on chaotic systems. For instance, Bisht et al. [5] proposed a new method that uses the four dimensional Lorenz system and bit-level permutation to present a color image encryption technique. Hua et al. [6] proposed a model for creating chaotic sequences in two dimensions that combine a sine map and a logistic map. Al Hasani [7] produced a chaotic optical signal using a semiconductor laser and optical feedback. Qian et al. [8] proposed a new color image

encryption method using chaotic maps in three-dimensional. Benyamin et al. [9] proposed a pseudorandom chaotic sequence created by a hyperchaotic system that used three-dimensional chaotic maps to scramble and permute processes. Liu et al. [10] proposed a four dimensional chaotic map and steganography-based image encryption algorithm. Anlin et al. [11] proposed a chaotic optical carrier-based opto-electronic oscillator, and used it to encrypt messages by chaos-masking scheme (CMS). Bao et al. [12] proposed bidirectional chaotic communication with WDM using semiconductor laser systems with concealing a time delay. Al-Saidi et al. [13][14] proposed a new 2D chaotic map to encrypt messages for a secure communication system. A new Lightweight AES utilizing a chaotic design is proposed by Fadhil et al. in [15]. Natiq et al. [16] proposed a new four dimension chaotic laser system; they studied its dynamics properties and complexity. Veeman et al. [17] proposed a new metastable chaotic oscillator; they assessed the complexity of their system by the sample entropy algorithm.

In this paper, a different channel spacing was analyzed using Dense Wavelength Division Multiplexing (DWDM). The eight-channels are transmitted through Single Mode Fiber (SMF), the performance is designed and analyzed with a 100 GHz (0.8 nm) spacing between each channel, from 193.1-193.8 THz. It is amplified utilizing Erbium-Doped Fiber Amplifier (EDFA) to compensate the optical channel attenuation, where the data was modulated using the Mach-Zehnder Modulator (MZM) to transmitting data for longer distances without losses. A post-dispersion compensation configuration is adopted using (DCF) Dispersion Compensating Fiber (DCF) to compensate for the dispersion of SMF. The modulation type is Non Return to Zero (NRZ), at a 10 Gb/s data rate and for NRZ signal transmission through fiber, 100 GHz spacing is simulated with eight users on the sender side and eight users on the receiver side. Each transmission results in an 80 Gbps high data rate transfer over 100 km, and range of the input signal power is from -15 dBm to 15 dBm with a 5 dBm step is numerically demonstrated. In addition, a new chaotic encryption scheme is used. The cipher signal is then transmitted at different fiber lengths (50 km, 75 km, 100 km, and 125 km). The The Q-factor, the BER, and the opening eye diagram are used to analyze and evaluate the performance measures of the proposed system.. It is noteworthy that The analysis of the system is performed based on the combination of simulation results obtained from MATLAB and the Optisystem 7 simulation program. This paper is organized into six parts; in addition to this introductory section, Section 2 presents a new secure cryptosystem based on chaotic design. Background about the Optisystem component is introduced in Section 3. Section 4 designed an 8-channel DWDM System. Section 5 discusses the result and analysis, and finally, Section 6 shows the conclusion that explains the benefit of the proposed system.

II. New secure cryptosystem based chaotic design

In this part, a new cryptosystem is proposed. The data (images) sent from the source was encrypted using a new Chaotic Stream Segmentation (CSS). The key is generated using a novel five-dimension chaotic system design. A plaintext or image is transformed into cipher text of the same size satisfied by hiding the plaintext with a keystream, utilizing a simple XOR operation in the diffusion process. Eight users are on the transmitter side and eight at the destination in this system.

2.1. The proposed chaotic system

A new 5D dynamical system is introduced as follows:

$$\begin{aligned} f(1) &= (y-w)u - x + ax; \\ f(2) &= (z-u)x - y + by; \\ f(3) &= (w-x)y - z + cz; \\ f(4) &= (u-y)z - w + dw; \\ f(5) &= (x-z)w - u + eu; \end{aligned} \tag{1}$$

where x, y, z, w, and u are the state variables, and Positive parameters include a, b, c, d, and e.

2.2. The algorithm of the proposed cryptosystem

A new algorithm for the encryption process is proposed. The 5D chaotic system is used to provide the key. It is known as the Chaotic Stream Segmentation (CSS) method.

The key generation and the encryption parts are presented as follows:

I. Key generating part

Key generating is the main part of any encryption scheme. When the keyspace is large, it is resulted in a highly secure system to resist a brute force attack. This property is achieved in this work because a chaos system is used to generate the key.

Input: the chaotic system (1)
Initial condition

$$k = \{x_{10}, x_{20}, x_{30}, x_{40}, x_{50}, a_0, b_0, c_0, d_0, e_0\}$$

Output: state as square arrangement, in which each pixel is 8 bits.

1. In each call, a different initial condition is used, which results in generating of a different state.
2. Solving system (1) to find the trajectories using the given initial conditions with the help of the 4-step Range Kutta method.
3. Iterate system (1) for *m* times to generate a chaotic sequence $X = \{x_1, x_2, \dots, x_m\}$.
4. Arrange the keystream generated by the system (1) in a matrix form with the same size of the given input such that, $S_{ij} = \sum_{L=1}^{5} x_{jL}$ when $i = 1, \dots, m$, and $j=1:5$.

II. Encryption part

Input: (image *P* of size *mxn*)
Output: Cipher image C

1. Generate S matrix, the same size as *P*

$$SP = XOR(S, P)$$

2. Do the following permutation to perform the diffused property
   a = sort SP in ascending order

I. Use the next steps to permute a:

```
For i = 1 to n
 For j = 1to m
  For k = 1 to m
   If a(j,i) = SP(k,i)
      t(j,i) = perm (k,i)
      k = m + 2
   End
   End k, end j,  end i
NSP = t
```

3. Partition NSP into four parts (SP_1, SP_2, SP_3, SP_4)
4. Generate four new states S_{ij}^{z}, z = 1,…,4, each with the same size of SP_i.
5. For i = 1: 4
   $ST_i = XOR(S^i, SP_i)$
   End
6. Merge the output of step 5 in one state arrangement such that:

$$OP = [ST_1, ST_2 \; ; \; ST_3, ST_4]$$

7. $C = OP$ % the cipher image

III. Optical communication system

Any form of communication that uses light rather than electrical current to carry messages is referred to as optical communication. Optical fibers are required for the transmission of signals during optical communication. The components of an optical communications system are a transmitter, a receiver, a light signal, and a transparent channel.

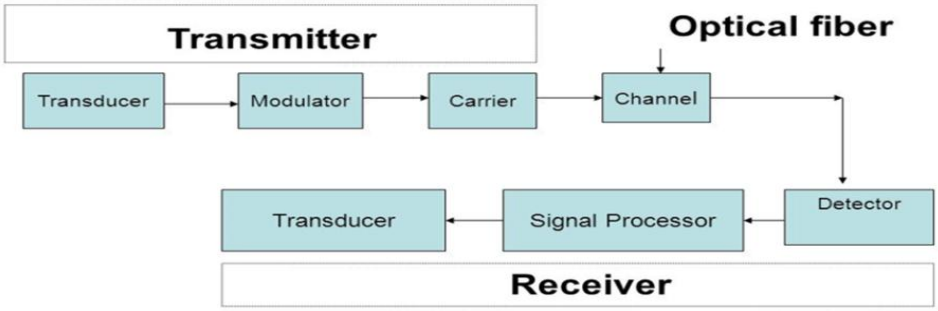

Figure 1: Block diagram of optical communication channel

3.1. Simulation component

Using the simulation program (Optisystem) increases the understanding of how each optical communication system works [18][19][20]. In addition, it makes it easier to assess design parameters than it would be to do physical experiments or analytical computations. The main component that is utilized in an Optisystem is present in Table 1.

Table1: Optical Fiber system components

	PARAMETERS	SPECIFICATIONS
Input data	Binary Null	Output (Signal type) = Binary
	MATLAB Component	Input =Binary signal
Transmitter part	CW LASER	Wavelength = 1550nm, Power=5dBm, Bandwidth= 10Gbps
	NRZ pulse Generator	Amplitude=5
	Mach-Zehner Modulator	Extinction ratio=30db
	WDM Mux 8x1	Bandwidth = 50 Ghz
Channel	SMF	Length=100km, Attenuation = 0.2dB/km
	DCF	Length = 15.22, Dispersion = -110 ps/ns/km, Attenuation = 0.44 dB/km
	EDFA	Gain = 31 dB, Wavelength = 980nm Noise figures= 3 dB
Receiving part	Photodetector PIN	Responsivity= 1 A/W
	Low pass Bessel filter	Cutoff frequency= 7.5 GHz
	3R Regenerator	
Measurements component	Oscilloscope Visualizer	
	Optical Spectrum Analyzer	
	BER Analyzer	
	WDM Analyzer	
	Dual port WDM Analyzer	
Data out	MATLAB Component	Output (Signal type) =Binary signal

IV. Design of 8-channel DWDM System

The Dense Wavelength Division Multiplexing technique is the best optical communication system for long-distance communication [21]. It increases the information-carrying capacity, includes multiplexing a range of wavelength signals onto a one fiber. Each fiber has a number of parallel optical channels, each fiber using a tiny different wavelength of light. The fibers use the wavelengths of light to send information either parallel-by -bit or serial-by-character. The most essential parts of any DWDM system are transmitters, receivers, EDFA, multiplexors, and de-multiplexors [22] [23].

In the OptiSystem model, eight optical channels were suggested, each capable of carrying 10 Gbits/sec. In Figure 2, a DWDM system is displayed. On the system's transmission side, optical signals are produced by eight CW lasers (193.1THz –193.8THz) operating with a power of 5 dBm in the 1550 nm region. These input signals are combined by the optical multiplexer (MUX) to produce a polychromatic output signal. It is subsequently sent for transmission through a single optical fiber. At the receiving end of the link, The MUX transmits the combined signal to the optical demultiplexer (DEMUX). The combined optical signal is split by the DEMUX into the native optical communication wavelengths. Figure 3 displays the signal's spectrum at the MUX output for an 8-channel multiplexed signal.

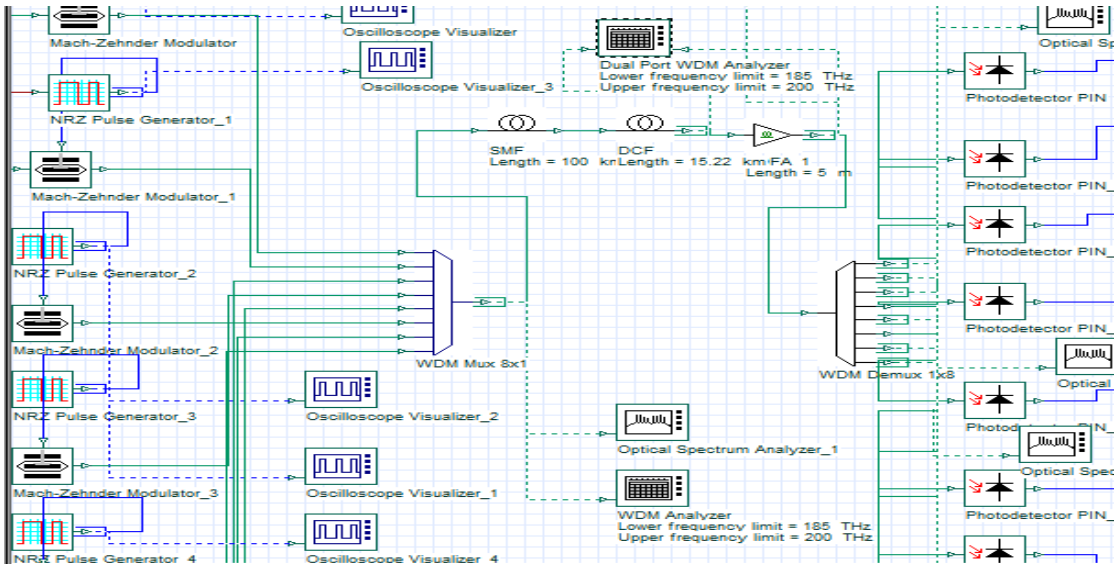

Figure 2: Fiber Optic DWDM system

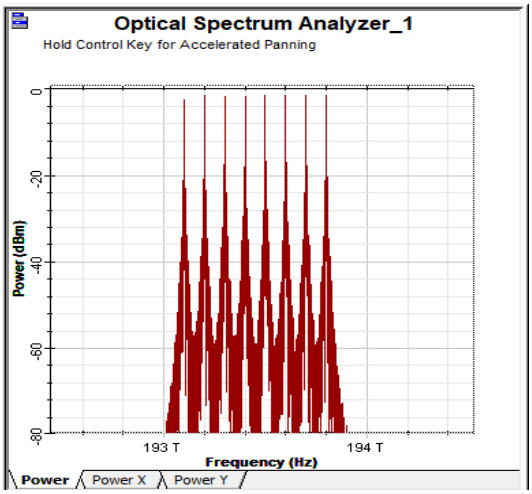

Figure 3: 8-channel multiplexed signal spectrum

4.1. Transmitter Module

Figure 4 shows the four components of the transmitter module. In order to produce the NRZ signal at 10Gbps, there are eight NRZ transmitters. The output of the MATLAB bit sequence generator is put into a pulse generator. An externally modulated LASER that runs at a wavelength of 1550 nm is modulated using NRZ pulses. The Mach-Zehnder Modulator is interferometric intensity modulator [24]. It implements a continuous wave (CW) laser. The output is sent to an eight-channel DWDM multiplexer with a line width of 10 MHz and a channel spacing of 0.8 nm.

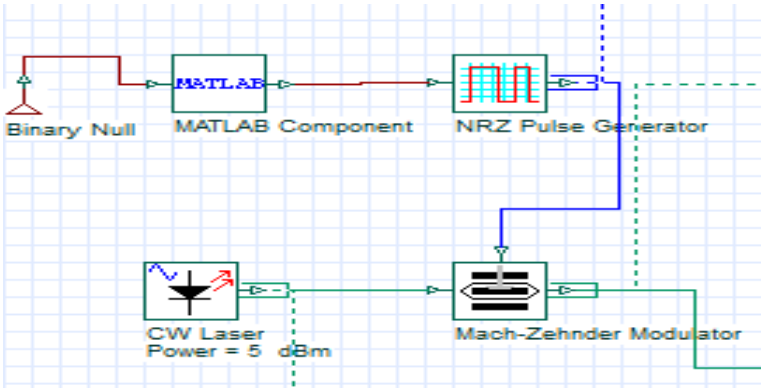

Figure 4: Transmitter design

4.2. Channel Design

The 8-channel DWDM Multiplexer's output is given to SMFs of lengths of 50 Km ,75 Km, 100 km, and 125 km with Post-dispersion compensated fiber of 15.22 km. The EDFA amplifiers are utilized with respective gains of 33dB to overcome the effect of attenuation [25]. Figure 5 shows the fiber link design of 100Km SMF.

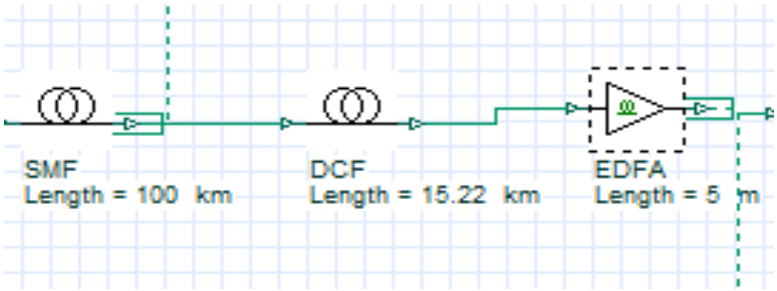

Figure 5: Fiber Design

4.3. Receiver Design

Firstly, the output from each channel is fed to the SMF. Next, the fiber's output is passed to an 8-channel DWDM demultiplexer (DMX). The receiver design in Figure 6 comprises of an SMF whose output is passed into a PIN photodetector with a response of 1 A/W and a dark current of 10 nA, It converts optical signals into electrical signals. The electrical signal is then sent through a Low Pass Bessel fourth order filter with a 0.75 Hz bandwidth and a depth of 100 dB. After that comes the 3R regenerator to regenerate an electrical signal, which is based on NRZ pulse generator and a data recovery component. It makes both the original bit sequence and a modulated electrical signal for BER analysis. The eye diagram is constructed using the output of the BER analyzer, which also gives the system's BER performance and Quality factor. The project's input and output are managed by the MATLAB code.

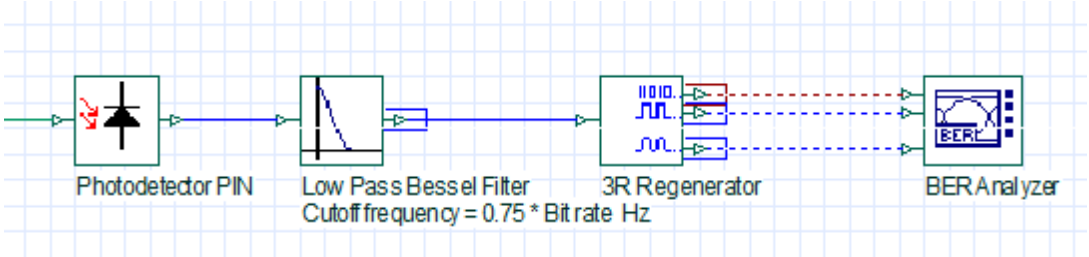

Figure 6: Receiver Design

4.4. Optical Amplifier Simulation

As indicated by their names suggest, light signals are amplified totally in the optical domain via optical amplifiers, eliminating the need for optical to electronic conversion. Long-haul fiber optic systems now require optical amplifiers as the demand for longer transmission lengths has increased.. Long-distance optical systems benefit from Erbium-doped fiber amplifiers (EDFAs), Raman optical amplifiers, and semiconductor optical amplifiers (SOAs), which reducing the effects of attenuation and dispersion [26]. The most well-known and common optical amplifier is EDFA for silica-based fibers with a low-loss optical window [27]. Erbium-doped fiber amplifiers (EDFAs) are a fundamental component of fiber optic systems due to the expansion of dense wavelength-division multiplexing (DWDM) applications. EDFAs enable the transmission of data over long distances without conventional repeaters. The EDFA is the most commonly used method in long-distance optical communication to compensate for optical fiber loss and increase optical transmission distance. The amplified effect can be observed from the simulation results. The optical spectrum is given in Figure 7.a without amplification, and the optical spectrum is shown in Figure 7.b after amplification.

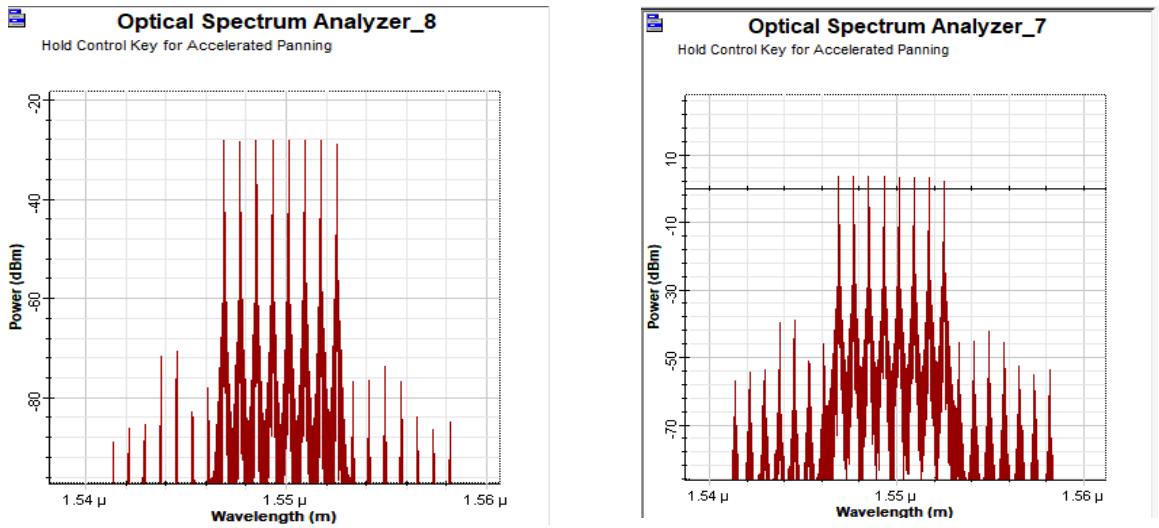

a. Before amplification b. After amplification

Figure 7: The optical signal spectrum before and after amplification.

Figure 7.a displays the 8-channel multiplexed signal's spectrum at the multiplexer's output before amplifying it. In contrast, Figure 7.b displays the 8-channel multiplexed signal's spectrum at the multiplexer's output after amplifying it. When the two graphs are compared, it is clear that the intensity value has gone up after amplification without changing the shape of the spectrum of optical signals. This shows that the system has done what optical amplification technology is supposed to do.

4.5. Dispersion Compensating Fiber (DCF) System Simulation

The DCF is the most widely used method for compensating for dispersion [28]. Using DCF in systems for long distance optically amplified fiber transmission,, it has been produced as one of the most useful methods for compensating for chromatic dispersion [29]. DCFs are specially made fibers having negative dispersion. Negative dispersion with a high value compensates for positive dispersion over significant lengths of SMFs. As displayed in Figure 4, a post-dispersion compensation technique is used by the dispersion compensating fiber of negative dispersion against the regular fiber to compensate for chromatic dispersion. Single mode fiber is ideal for long-distance, high-capacity optical fiber communications. The SMF has a 16.75 ps/nm/km dispersion in the 1550 nm window. As a result, using DCF to improve installed single-mode fiber lines is a good idea.

V. Results and Analysis

5.1 Results of proposed system design using different power

We will analyze the impact of input launch power from -15 to 15 on signal performance when the signal is traveling through SMF for 100 km of optical fiber length. The Q-factor vs. power is shown in Figure 8 (a), and the log BER vs. power is shown in Figure 8(b). Figure 8(c) show Q-factor and Log BER vs. Power. The Q-factor and BER showed acceptable results for powers > 0 dBm with values of 42 of the Q-factor and 0 for BER, at a fiber of length 100 km and a power of 5 dBm. Additionally, the increase in the input signal to 15 dBm damaged the eye shape, decreased the Q-factor to 10, and increased the minimum log of BER to -24, but these values are still acceptable.

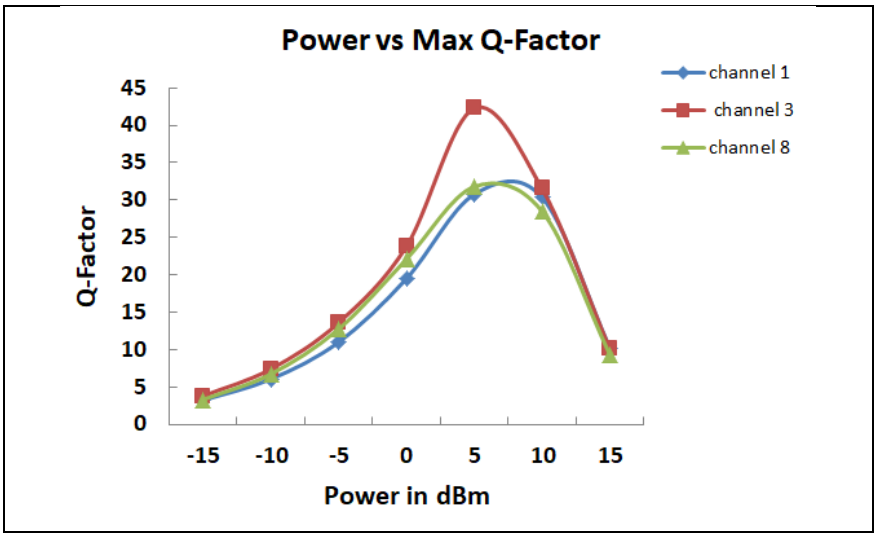

Figure 8(a). Q-factor vs. Power

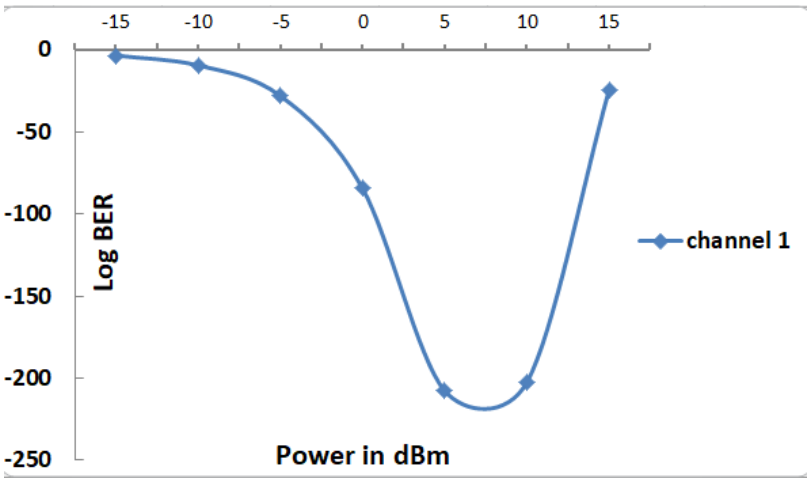

Figure 8(b). Log BER vs. Power

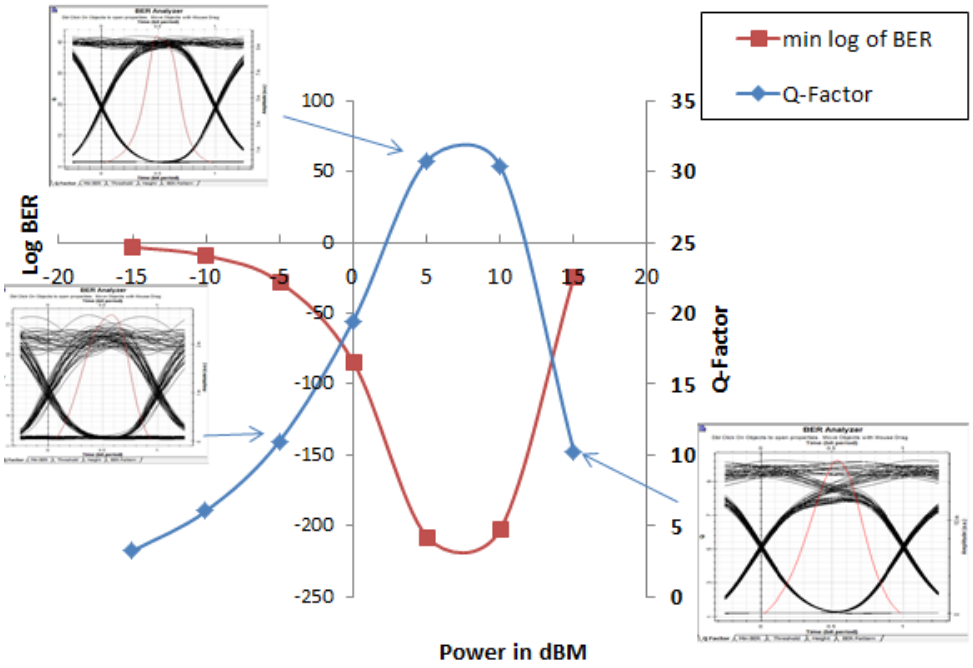

Figure 8(c). The Q-factor and Log BER vs. Power

The BER values are analyzed, the acceptable value is taken at channel 3 for the BER 0 at the rate of data of 10 Gbps and power of 5 dBm, for length of 100 km as shown in Table 2.

Table 2. Comparison table of BER analysis at different power

Power	Channel 1		Channel 3		Channel 8	
	Q-factor	BER	Q-factor	BER	Q-factor	BER
-15	3.22923	0.000458	3.78845	6.15389e-005	3.31235	0.000353
-10	6.04691	4.77E-10	7.38558	5.46817e-014	6.71985	6.16E-12
-5	10.9862	1.30E-28	13.5822	1.67055e-042	12.7286	1.26E-37
0	19.4655	5.97E-85	23.7664	2.34582e-125	22.0755	1.56E-108
5	30.7621	2.35E-208	42.2797	0	31.7859	2.73E-222
10	30.3699	3.77E-203	31.5554	4.3947e-219	28.5127	2.16E-179
15	10.2395	3.55E-25	10.0816	1.88162e-024	9.32913	2.95E-21

5.2 Results of proposed system design using different distance 50, 75,100 and 125 km fiber length with power of 5 dbm.

The performance of the Q-factor is shown in Figure 9, as fiber length increases, the Q-factor reduces and BER also increases as the transmission distance increases. The performance is dependent on system parameters in the Optisystem simulation by changing the optical fiber length from 50km to 125km. The Q-factor and BER values are evaluated as displayed in Table 3.

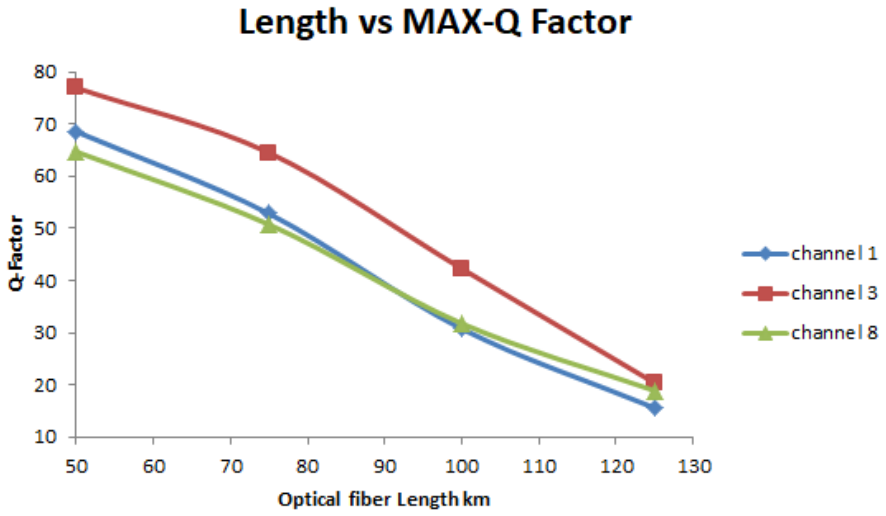

Figure 9. Q-factor vs. distance with power equal to5 dBm

Table 3. Q-factor and BER for various distance

	50 km length		75 km length		100 km length		125 km length	
	Q-Factor	BER	Q-Factor	BER	Q-Factor	BER	Q-Factor	BER
Ch1	68.5472	0	52.8215	0	30.7621	2.35068E-208	15.6187	1.53475E-55
Ch2	73.4043	0	61.3809	0	36.1785	3.93069E-287	15.9062	1.66399E-57
Ch3	76.9323	0	64.5006	0	42.2797	0	20.3918	6.27727E-93
Ch4	59.6867	0	47.2187	0	30.1055	1.23489E-199	15.376	6.99648E-54
Ch5	66.8459	0	52.9765	0	33.1201	4.59403E-241	17.0094	2.07137E-65
Ch6	64.7205	0	57.3665	0	38.4321	9.88131e-324	18.6319	5.40311E-78
Ch7	71.9285	0	50.5767	0	36.7587	2.64058E-296	17.2121	6.17393E-67
Ch8	64.6953	0	50.7465	0	31.7859	2.73398E-222	18.918	2.40194E-80

We describe the Eye diagram for 50, 75, 100 and 125 km optical length for Q factor and BER.

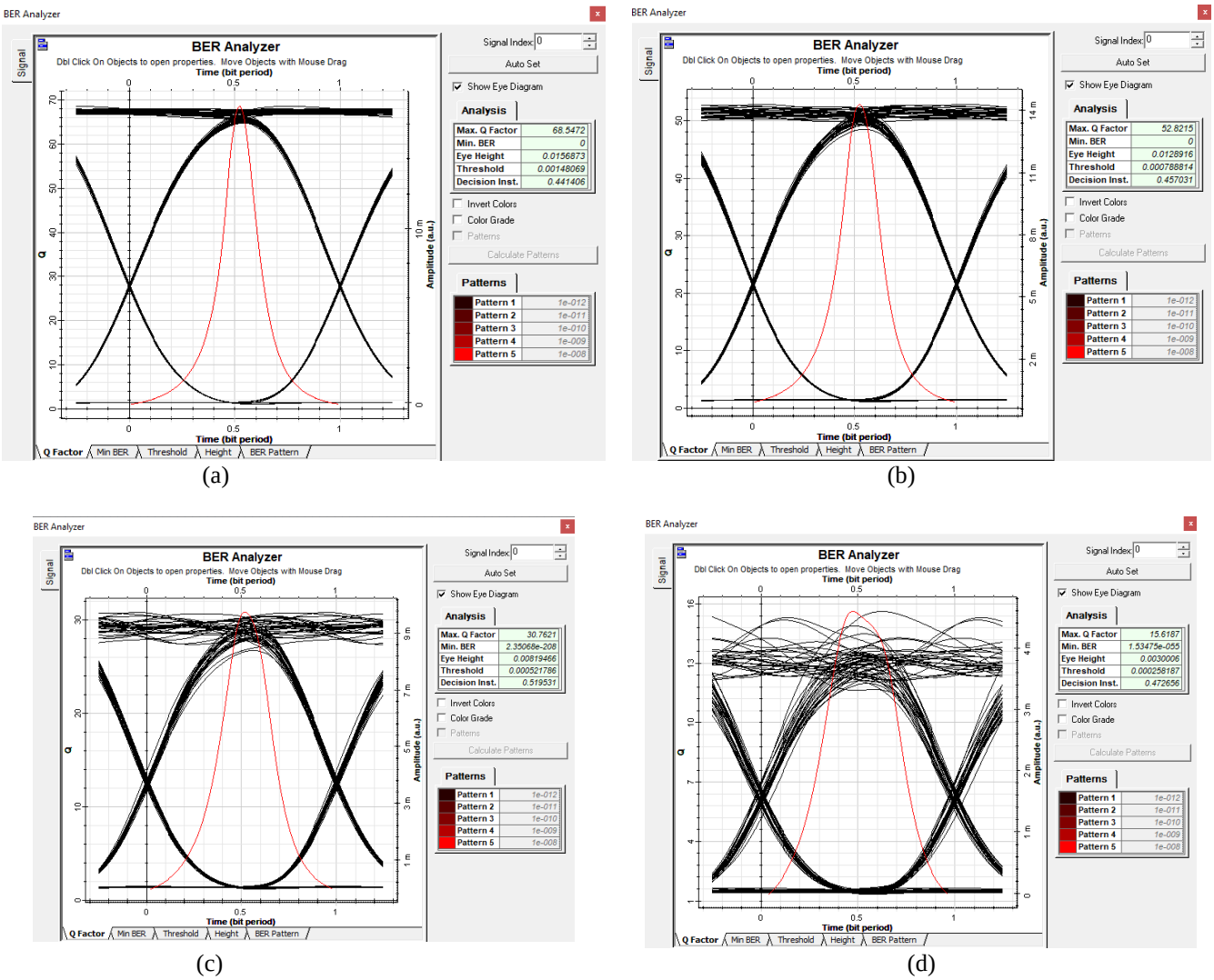

Figure 10: (a) Eye diagram for 50 km length, (b) Eye diagram for 75 km length, (c) Eye diagram for 100 km length, (d) Eye diagram for 125 km length

From the table and eye diagram, it is clear that as fiber length increases, BER increases as the transmission distance increases.

5.3 Result of the proposed (CSS) method

The result of the encryption and decryption system for different types of images (gray scale and color images) is shown in Figure 11.

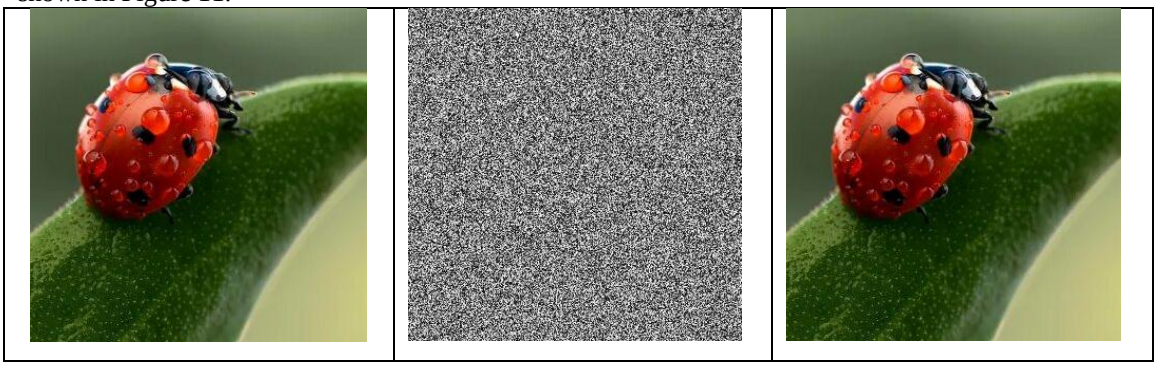

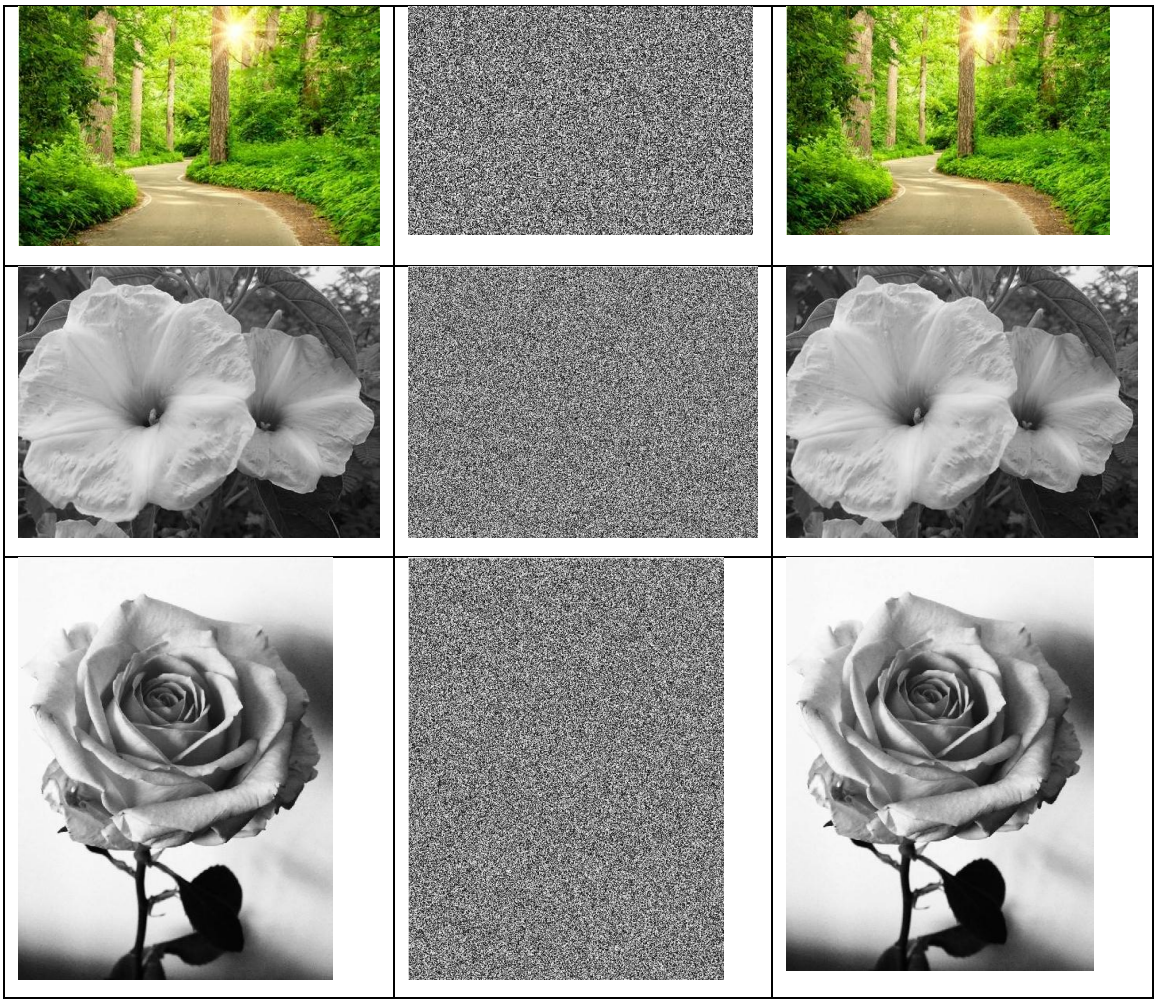

(a) (b) (c)

Figure 11: The simulation results of a cryptosystem CSS: (a) grayscale and Color plain images; (b) cipher images of (a); (c) decryption of (b)

5.3.1 Histogram

An image histogram is a graph that displays the number of pixels in an image at each different intensity value.

For example, Figure 12 displays the histogram of the plain images, the encrypted images, and the image after decryption.

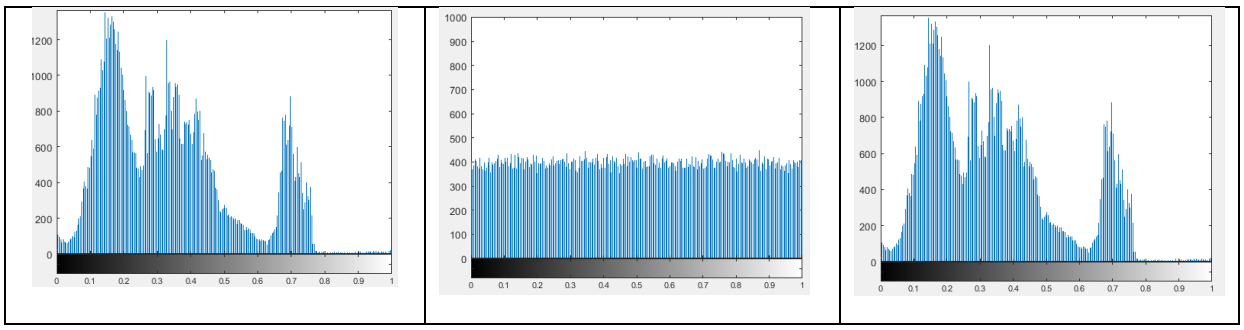

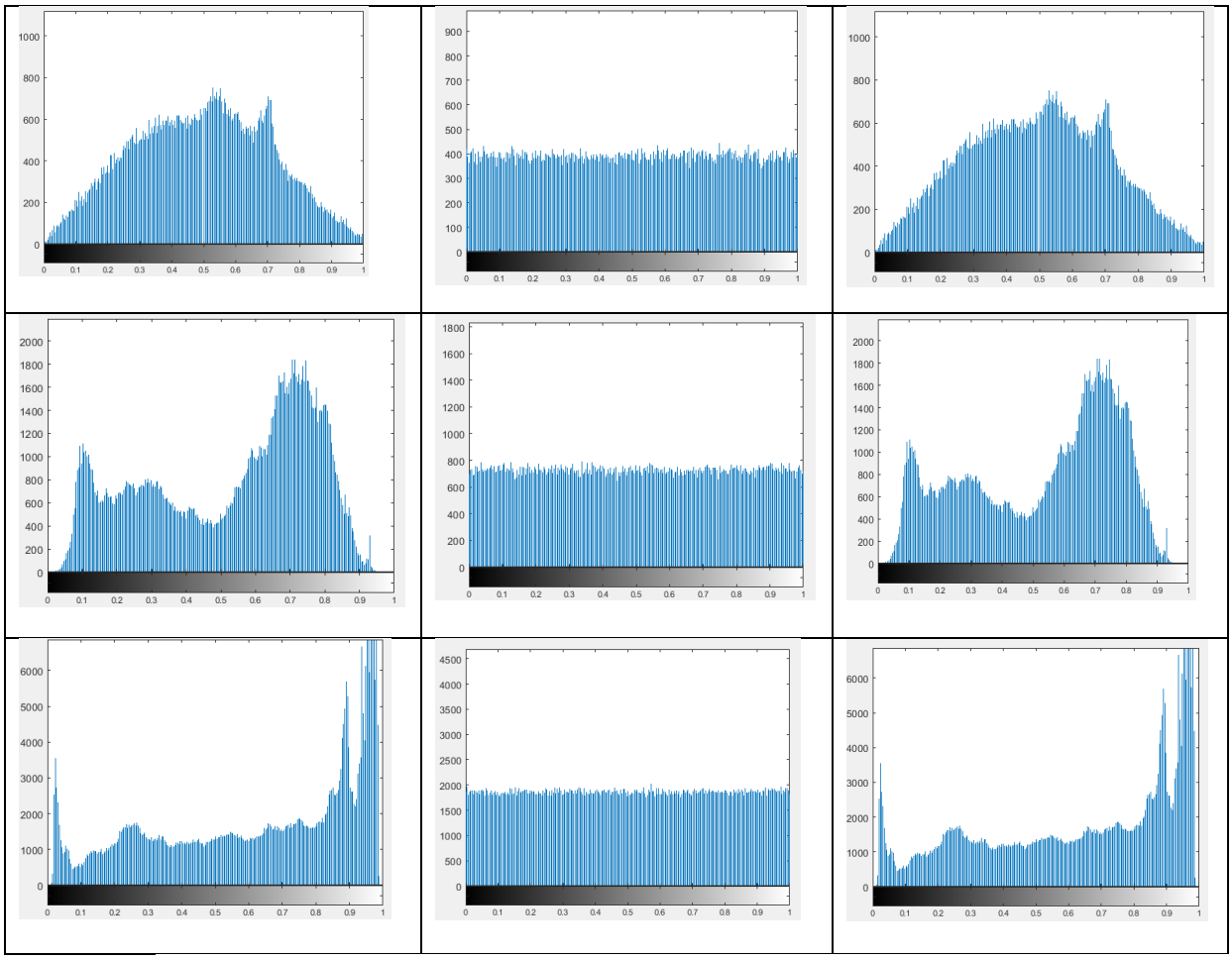

(a) (b) (c)

Figure 12: (a) Histogram for plain image, (b) Histogram of cipher image (c) Histogram of decryption image

When displayed, the histogram of the input image obviously, the encrypted image's histogram differs significantly from the histograms of the original photos, and the histogram of the image after decryption is the same as the histogram of the plain image. So, we can say that the suggested algorithm works efficiently and cannot be broken by statistical attacks.

(b) CONCLUSION

This paper analyzed the effect of input signal power range of -15 to 15 with a step of 5 dBm, on the Q-factor and BER performance, and examining the suggested system under different lengths of fiber with an optimum input signal power of 5 dBm. An encoded signal based on a 5D chaotic system is tested through an 80 Gb/s DWDM optical comminications system. Post-DCF and optical amplifiers have been employed to compensate for power loss and the dispersion of the optical channel. The signal is transmitted through a 100 km range at a 10 Gb data rate. Simulation results from MATLAB and the Optisystem 7 simulation software are analyzed and optimized in term of input signal power and fiber length.

References

[1] L. Yi, T. Zhang, Z. Li, J. Zhou, Y. Dong, and W. Hu, “Secure optical communication using stimulated Brillouin scattering in optical fiber,” *Opt. Commun.*, vol. 290, pp. 146–151, 2013.

[2] Y. Frauel, A. Castro, T. J. Naughton, and B. Javidi, “Resistance of the double random phase encryption

against various attacks," *Opt. Express*, vol. 15, no. 16, pp. 10253–10265, 2007.

[3] Z. Gao *et al.*, "40Gb/s secure optical communication based on symbol-by-symbol optical phase encryption," *IEEE Photonics Technol. Lett.*, vol. 32, no. 14, pp. 851–854, 2020.

[4] B. P. Alapatt, A. Kavitha, and J. Amudhavel, "A novel encryption algorithm for end to end secured fiber optic communication," *Int. J. Pure Appl. Math.*, vol. 117, no. 19 Special Issue, pp. 269–275, 2017.

[5] A. Bisht, M. Dua, S. Dua, and P. Jaroli, "A color image encryption technique based on bit-level permutation and alternate logistic maps," *J. Intell. Syst.*, vol. 29, no. 1, pp. 1246–1260, 2020.

[6] Z. Hua, F. Jin, B. Xu, and H. Huang, "2D Logistic-Sine-coupling map for image encryption," *Signal Processing*, vol. 149, pp. 148–161, 2018.

[7] M. H. Al Hasani and K. A. M. Al Naimee, "Quantum Key Distribution and Chaos Bandwidth Effects on Impact Security of Quantum Communications," *Iraqi J. Sci.*, pp. 1266–1273, 2019.

[8] X. Qian, Q. Yang, Q. Li, Q. Liu, Y. Wu, and W. Wang, "A novel color image encryption algorithm based on three-dimensional chaotic maps and reconstruction techniques," *IEEE Access*, vol. 9, pp. 61334–61345, 2021.

[9] B. Norouzi, S. Mirzakuchaki, S. M. Seyedzadeh, and M. R. Mosavi, "A simple, sensitive and secure image encryption algorithm based on hyper-chaotic system with only one round diffusion process," *Multimed. Tools Appl.*, vol. 71, no. 3, pp. 1469–1497, 2014.

[10] J. Liu, Y. Wang, Q. Han, and J. Gao, "A Sensitive Image Encryption Algorithm Based on a Higher-Dimensional Chaotic Map and Steganography," *Int. J. Bifurc. Chaos*, vol. 32, no. 01, p. 2250004, 2022.

[11] L. Jiang *et al.*, "Trading off security and practicability to explore high-speed and long-haul chaotic optical communication," *Opt. Express*, vol. 29, no. 8, pp. 12750–12762, 2021.

[12] X. Bao, Q. Li, T. Wu, Y. Deng, M. Hu, and R. Zeng, "WDM-based bidirectional chaotic communication for semiconductor lasers system with time delay concealment," *Opt. Commun.*, vol. 472, p. 125868, 2020.

[13] N. M. G. Al-Saidi, D. Younus, H. Natiq, M. R. K. Ariffin, M. A. Asbullah, and Z. Mahad, "A new hyperchaotic map for a secure communication scheme with an experimental realization," *Symmetry (Basel).*, vol. 12, no. 11, p. 1881, 2020.

[14] D. Younus, N. M. G. Al-Saidi, and W. K. Hamoudi, "Secure optical communication based on new 2D-hyperchaotic map," in *AIP Conference Proceedings*, 2019, vol. 2183, no. 1, p. 90006.

[15] M. S. Fadhil, A. K. Farhan, M. N. Fadhil, and N. M. G. Al-Saidi, "A New Lightweight AES Using a Combination of Chaotic Systems," in *2020 1st. Information Technology To Enhance e-learning and Other Application (IT-ELA*, 2020, pp. 82–88.

[16] H. Natiq, M. R. M. Said, N. M. G. Al-Saidi, and A. Kilicman, "Dynamics and complexity of a new 4d chaotic laser system," *Entropy*, vol. 21, no. 1, p. 34, 2019.

[17] D. Veeman, H. Natiq, N. M. G. Al-Saidi, K. Rajagopal, S. Jafari, and I. Hussain, "A new megastable chaotic oscillator with blinking oscillation terms," *Complexity*, vol. 2021, 2021.

[18] S. R. Tahhan, A. K. Abass, and M. H. Ali, "Characteristics of chirped fiber bragg grating dispersion compensator utilizing two apodization profiles," *J. Commun.*, vol. 13, no. 3, 2018, doi: 10.12720/jcm.13.3.108-113.

[19] F. Abdullah, M. Z. Jamaludin, M. H. Ali, M. H. Al-Mansoori, A. K. Abass, and T. F. Al-Mashhadani, "Influence of Raman Pump Direction on the Performance of Serial Hybrid Fiber Amplifier in C + L-Band," in *2018 IEEE 7th International Conference on Photonics (ICP)*, 2018, pp. 1–3.

[20] S. H. Alnajjar, M. H. Ali, and A. K. Abass, "Enhancing Performance of Hybrid FSO/Fiber Optic Communication Link Utilizing Multi-Channel Configuration," *J. Opt. Commun.*, 2019, doi: 10.1515/joc-2018-0193.

[21] S. Singh and R. S. Kaler, "Investigation of hybrid optical amplifiers with different modulation formats

for DWDM optical communication system," *Optik (Stuttg).*, vol. 124, no. 15, pp. 2131–2134, 2013.

[22] S. M. Abdulsatar, M. A. Saleh, A. K. Abass, M. H. Ali, and M. A. Yaseen, "Bidirectional hybrid optical communication system based on wavelength division multiplexing for outdoor applications," *Opt. Quantum Electron.*, vol. 53, no. 10, pp. 1–11, 2021.

[23] A. A. Khadir, B. F. Dhahir, and X. Fu, "Achieving optical fiber communication experiments by optisystem," *Int. J. Comput. Sci. Mob. Comput.*, vol. 3, no. 6, pp. 42–53, 2014.

[24] T. Hiraki *et al.*, "Integration of a high-efficiency Mach-Zehnder modulator with a DFB laser using membrane InP-based devices on a Si photonics platform," *Opt. Express*, vol. 29, no. 2, pp. 2431–2441, 2021.

[25] S. Lawan, M. Ajiya, and D. Shu'Aibu, "Numerical simulation of chromatic dispersion and fiber attenuation in a single-mode optical fiber system," *Signal*, vol. 10, no. 10, p. 3, 2012.

[26] M. H. Ali, F. Abdullahi, M. Z. Jamaludini, M. H. AI-Mansoori2, T. F. AI-Mashhadani, and A. K. Abassi, "Effect of EDF Position on the Performance of Hybrid Dispersion-Compensating Raman/EDF Amplifier," in *4th International Conference in Photonics (ICP)*, 2013, pp. 187–189. Accessed: Jun. 28, 2014. [Online]. Available: http://ieeexplore.ieee.org/xpls/abs_all.jsp?arnumber=6687109

[27] L. Sirleto and M. A. Ferrara, "Fiber amplifiers and fiber lasers based on stimulated Raman scattering: a review," *Micromachines*, vol. 11, no. 3, p. 247, 2020.

[28] N. S. Effendi, Y. Natali, and C. Apriono, "Study of Dispersion Compensation with Dispersion Compensating Fiber in 10 Gbps Single-Mode Fiber," in *2021 International Conference on Green Energy, Computing and Sustainable Technology (GECOST)*, 2021, pp. 1–6.

[29] S. R. Tahhan, M. H. Ali, and A. K. Abass, "Characteristics of Dispersion Compensation for 32 Channels at 40 Gb/s under Different Techniques," *J. Opt. Commun.*, vol. 41, no. 1, pp. 57–65, 2017, doi: 10.1515/joc-2017-0121.